

# Flower-like TiO<sub>2</sub> Nanostructures: Synthesis, Characterization and Photocatalytic Properties

Yinye Li<sup>1</sup>, Jun Fan<sup>1,\*</sup>, Xiaoyun Hu<sup>2</sup>, Enzhou Liu<sup>1</sup>, Xiao Fan<sup>1</sup>, Huitong Wu<sup>1</sup>, Yongning Ma<sup>1</sup>, Chunni Tang<sup>1</sup>

<sup>1</sup>School of Chemical Engineering, Northwest University, No. 229 Taibai North Road, Xi'an, Shannxi, 710069, P. R. China.

<sup>2</sup>Department of Physics, Northwest University, No. 229 Taibai North Road, Xi'an, Shannxi, 710069, P. R. China.

\*E-mail: fanjun@nwu.edu.cn, Tel: +8613110493201

## ABSTRACT

Flower-like TiO<sub>2</sub> materials, with their advantages of high specific surface area, large pore structure, and high photocatalytic activity, have been widely used in environmental management, air purification, and surface self-cleaning. TiO<sub>2</sub> nanoflowers were prepared by a hydrothermal method. Ag-doped TiO<sub>2</sub> nanostructures are obtained using microwave-assisted reduction. Results show that Ag are well dispersed on the surface of TiO<sub>2</sub>, which can enhance the visible absorption. Ag/TiO<sub>2</sub> could also restrain the recombination of photo-generated electron-hole pairs efficiently. The results of photocatalytic water splitting showed that Ag/TiO<sub>2</sub> samples had better photocatalytic performance than pure TiO<sub>2</sub>.

**Keywords:** Flower-like TiO<sub>2</sub>; hydrothermal synthesis; nanostructures; Photocatalysis.

## 1 INTRODUCTION

In recent decades TiO<sub>2</sub> materials attract significant attention for application in the heterogeneous photocatalysis<sup>[1-4]</sup> gas sensors<sup>[5-6]</sup> solar cells, and electrochromic devices. A lot of investigations have focused on TiO<sub>2</sub> photocatalysts due to their relatively high reactivity and chemical stability features. However, TiO<sub>2</sub> has a relatively wide band that requires ultraviolet (UV) light for activation, and UV light constitutes only about 4% of the sunlight spectrum. Besides, TiO<sub>2</sub> has a high recombination rate of electron-hole pairs during the photocatalysis process, leading to a lower photocatalytic efficiency. Therefore, a lot of efforts have been paid to synthesize TiO<sub>2</sub> nanostructures. This paper used a strategic hydrothermal synthesis of 3D TiO<sub>2</sub> nanostructures with well-defined shape and size. The existence of a large number of nanorods in the obtained 3D structures is important for improving the photochemical performance of TiO<sub>2</sub><sup>[7]</sup>. The key in the study for tuning the morphology and size of TiO<sub>2</sub> nanostructures is to control the temperature. Flower-like TiO<sub>2</sub> nanostructures, which are fabricated from oleic acid through a hydrothermal method, have seldom been reported. Furthermore, it has been proven that the growth of nanostructures as well as their properties significantly depends on the preparation process<sup>[8-15]</sup>. In this paper, TiO<sub>2</sub> microspheres assembled with ordered rutile

nanorods were synthesized in nonpolar solvent. Despite the extensive reports on nanostructures of crystalline anatase titania the organization of primary building units into three-dimensional nanostructures with a high surface area and their applications<sup>[16]</sup>. The effects of various experimental parameters, including reaction temperatures and the reactant concentrations and photocatalytic properties were studied.

## 2 EXPERIMENT

### 2.1. Preparation

In a typical experiment, 8 mL of titanium butoxide were added slowly into a 4 mL of concentrated HCl (36.5%). Then 40 mL of oleic acid were then added into the mixture under magnetic stirring. After the mixture was stirred for 3 h at room temperature, the solution was transferred into a Teflon lined autoclave of 100 mL capacity and heated at temperature 130°C, 150°C, 180°C for 12 h. The system was then allowed to cool to ambient temperature. The obtained product was collected by a vacuum filter and were collected through washing several times with pure ethanol to remove any possible organic solvent. At last, the products were dried in a vacuum at 60°C for 10 h, calcined at 450°C for 2 h, and the obtained white TiO<sub>2</sub> powders were ready for further characterization. Ag/TiO<sub>2</sub> was obtained by a microwave-assisted chemical reduction process. 0.5 g of polyvinylpyrrolidone (PVP, K30) was dissolved in 20 ml diethylene glycol (DEG) at room temperature and stirred for 6 h. Then NaH<sub>2</sub>PO<sub>2</sub>·H<sub>2</sub>O was added into the solution. Subsequently, 20 ml of AgNO<sub>3</sub> aqueous solution was added into the above solution, which was kept stirring for 20 min, then TiO<sub>2</sub> products was put into above solution. Then was exposed to microwave irradiation for 5 min at 140°C. We have generated three dimensional (3D) anatase titania nanostructures on surfaces.

### 2.2 Characterization

The samples were identified by X-ray diffractometer (Shimadzu, XRD-6000, Cu K $\alpha$  radiation). The morphology of the samples was observed using a scanning electron microscope (Hitachi S-4800). Photoluminescence spectra Times or Times Roman is were measured by fluorescence

spectrometer (Hitachi, F-7000). The absorption property of the samples was recorded using UV-vis spectrophotometer (Shimadzu, UV-3600).

### 3 RESULTS AND DISCUSSION

#### 3.1. Structure and morphology

Figure 1 illustrates the morphology of TiO<sub>2</sub> nanoflowers and Ag deposited TiO<sub>2</sub> nanoflowers. A small quantity of products can be finally obtained after the calcination process. The size, morphology as shown in (Figure 1), the generated products display three-dimensional morphology with a uniform size distribution. Fig. 1a, the temperature is so low that the morphology wasn't successfully formed. With increasing of the reaction the microspheres aggregated and larger quasi-spherical structures are formed. As the temperature rising, the nanorods grew slowly, the microspheres aggregated and larger spherical structures are formed (Fig. 1b). At 150°C, the products have a flower-like structure, which is composed of a lot of nanorods. HCl led to the growth of microspheres composed of rutile nanorods. The inset of (Fig. 1c) shows the presence of thick and fast packed nanorods. With the reaction temperature rises to 180°C, the nanorod density obviously increases. With the reaction temperature increasing, the crystallinity enhanced. Fig. 1d shows Ag on the surface of TiO<sub>2</sub> nanoflowers are obtained by microwave-assisted reduction of Ag(NO<sub>3</sub>)<sub>2</sub>. The presence of Ag does not damage the morphology of TiO<sub>2</sub> nanoflowers. Most of Ag are distributed on the surface of the spherical.

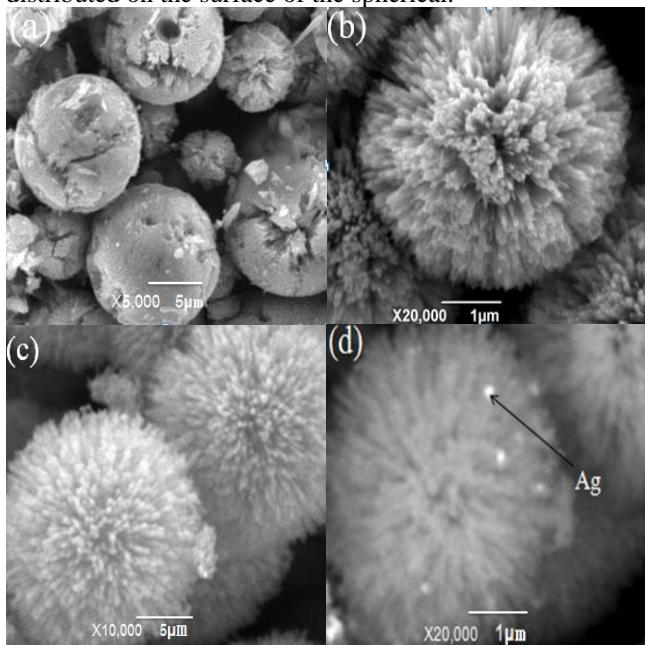


**Fig.1** SEM images (a) T=130°C (b) T=150°C (c) T=180°C (d) Ag/TiO<sub>2</sub> nanoflowers (T=180°C)

#### 3.2. X-ray Analysis

The XRD patterns of the products are shown in Fig. 2 from where we can see that the products have the same crystal structure of the phase. The XRD peaks arising at  $2\theta=25.1$  corresponds to (101) flat of anatase TiO<sub>2</sub> (JCPDS 21-1272), while the XRD peaks appears at 27.1, 35.9, 40.9, 54.0, 56.2 correspond to (110), (101), (111), (211), (220) planes of rutile TiO<sub>2</sub> (JCPDS 21-1276). The other peak at 38.1° ascribed to Ag (111) plane, and it is covered up by the peak at 38.4°, at the same time part of the diffraction peak still can be observed. Other three peaks at 44.3°, 64.4° and 77.5° attributed to Ag(200), (220), (311) planes can be seen clearly in the XRD patterns. The presence of Ag in the products obtained from the reduction of Ag<sup>+</sup>. In (Fig. 2a) there is no diffraction peak of Ag appears, which is because there is no AgNO<sub>3</sub>. No diffraction peak of Ag appears in (Fig. 2b), which may be related to the low concentration of AgNO<sub>3</sub> solution during the process. In (Fig. 2c) the concentration of AgNO<sub>3</sub> is higher than Fig. 2b, from which we can see the diffraction peak is sharper. With the reaction concentration increasing, the diffraction peaks slowly become sharper and narrower, which indicate the enhancement of crystallinity and growth of nanocrystals at higher concentration.

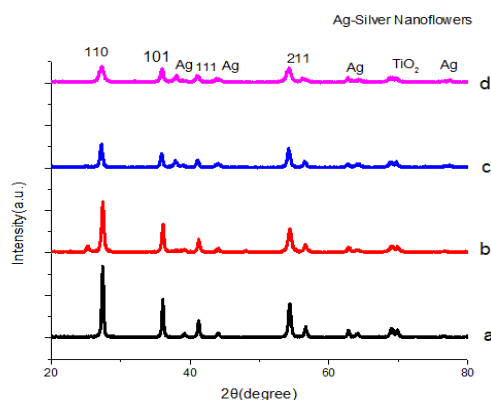


**Fig. 2** XRD patterns: (a) pure TiO<sub>2</sub>, (b) 0.001 mol/L Ag/TiO<sub>2</sub>, (c) 0.002 mol/L Ag/TiO<sub>2</sub>, (d) 0.003 mol/L Ag/TiO<sub>2</sub>

#### 3.3 UV-vis Analysis

UV-vis absorption spectra of the selected spherical assemblies of TiO<sub>2</sub> nanostructures are shown in the flowing Figure 3. The optical absorption spectra indicate that all the samples have the absorption edge at around 400 nm. The sample shows a strong absorption peak in the UV regime. The results and observations are in accordance with previously reported data from other teams [17-18]. We can see the absorption peaks are wide band gap semiconductors from the micrometer-scale spherical samples and anatase titania nanostructures. The absorption of the flower-like TiO<sub>2</sub> nanostructure is stronger than that of P25, it is because the flower-like TiO<sub>2</sub> nanostructures are porous structure and have large specific surface area, which is favor for

obtaining light attributed to multiple scattering of light [19-21]. Comparing with pure TiO<sub>2</sub>, the absorption of Ag/TiO<sub>2</sub> increases obviously in the visible region attributed to the SPR effect. Significantly, their light absorption edges of Ag/TiO<sub>2</sub> move obviously with a red shift to visible light extent compared with pure TiO<sub>2</sub>. The samples of Ag doped TiO<sub>2</sub> shows better visible light absorption activity. The interspaces between the flowerlike rods can regard as a light-transfer path for importing light into the internal TiO<sub>2</sub>, which allow light waves to penetrate deeply inside the TiO<sub>2</sub>. With the AgNO<sub>3</sub> concentration increasing, the peaks slowly become higher.

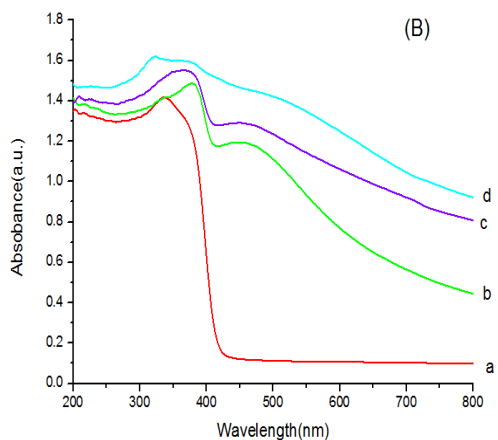
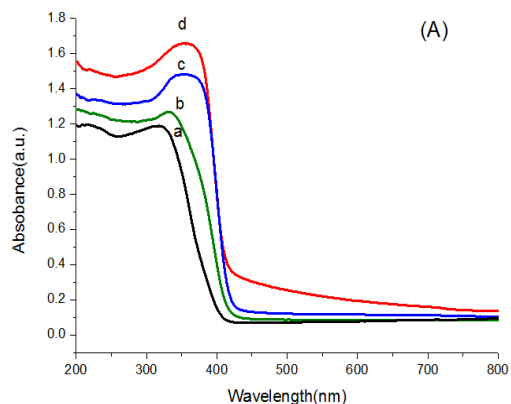


**Fig. 3** UV-vis spectra:  
A. (a) P25, (b) T=130°C, (c) T=150°C, (d) T=180°C  
B. (a) pure TiO<sub>2</sub>, (b) 0.001 mol/L Ag/TiO<sub>2</sub>,  
(c) 0.002 mol/L Ag/TiO<sub>2</sub>, (d) 0.003 mol/L Ag/TiO<sub>2</sub>,

### 3.4 Photoluminescence (PL) emission spectrum

Photoluminescence (PL) emission spectrum is a significant pathway to research the workpiece ratio of charge carrier trapping, immigration, and transfer [22]. As we all known that PL emission mainly results from the recombination of motive electron-hole pairs. When the emission intensity is lower, which indicates the decrease of recombination rate. The emission spectra of samples were

recorded under 290 nm excitation. As Fig. 4 shows, the emission spectra of Ag/TiO<sub>2</sub> samples seems to be similar with pure TiO<sub>2</sub>, which means that the loading of Ag has not induced new photoluminescence. In Fig. 4, there are two main emission peaks at 400 nm (3.10 eV) and 470 nm (2.67 eV). The peaks are assigned to electronic transition from the bottom of the conduction band to the top of the valence band and the defect levels formed by oxygen vacancies. The spectrum of curve a and b are weakened after Ag loading, which indicate the recombination of photogenerated electrons and holes is suppressed effectively.

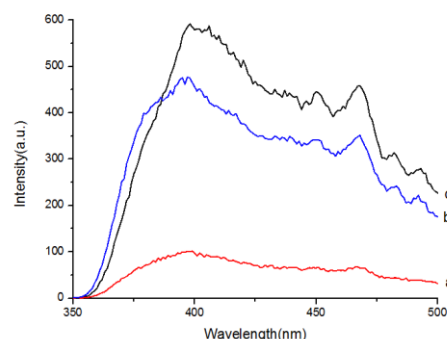


**Fig. 4** PL spectra: (a) 0.001 mol/L Ag/TiO<sub>2</sub>,  
(b) T=150 °C, (c) P25.

### 3.5 Photocatalytic water splitting

Photocatalytic water splitting to produce hydrogen was used to evaluate the activity of Photocatalysis using ethanol as a agent. In Fig. 5 the curve b, c and d are the hydrogen evolution rate of Ag/TiO<sub>2</sub> irradiated by UV and visible light, comparing with the curve a the hydrogen evolution rate were higher than the pure TiO<sub>2</sub>, which can be found that Ag/TiO<sub>2</sub> products performed better photocatalytic activity than pure TiO<sub>2</sub> under UV light irradiation. This improvement results from that the loaded Ag restrained the recombination of electron-hole pairs.

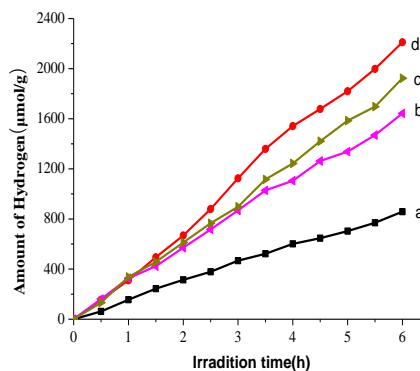


**Fig. 5** Hydrogen evolution: (a) TiO<sub>2</sub> (b) 0.001 mol/L Ag/TiO<sub>2</sub>, (c) 0.002 mol/L Ag/TiO<sub>2</sub>,  
(d) 0.003 mol/L Ag/TiO<sub>2</sub>

## 4 CONCLUSIONS

TiO<sub>2</sub> nanoflowers loaded with Ag nanoparticles were prepared by titanium butoxide and oleic acid using hydrothermal synthesis. The absorption in the visible region is significantly enhanced due to the content of Ag nanoparticles. Besides Ag can also restrain the recombination of photo-generated electron-hole pairs. The experiment indicated that the hydrogen evolution rate of Ag/TiO<sub>2</sub> samples irradiated by UV and visible light improved in various degrees compared with pure TiO<sub>2</sub>, the hydrogen evolution rate of Ag /TiO<sub>2</sub> is higher than that of pure TiO<sub>2</sub>. The nanostructures exhibit high photocatalytic activities.

## 5 ACKNOWLEDGEMENTS

This work supported by the National natural Science Foundation of China (No. 21306150, No. 21176199 and No. 51372201), the Shaanxi Provincial Research Foundation for Basic Research, China (No. 2013JQ2003, No. 2011JM1001 and No. 2012JM1020), the Scientific Research and Industrialization Cultivation Foundations of Education Department of Shaanxi Provincial Government, China (No. 2013JK0693 and No. 2011JG05), the Scientific Research Foundation of Northwest University (No. 12NW19), and the Scientific Research Staring Foundation of Northwest University (No. PR12216).

## REFERENCER

- [1] Han, X. G.; Kuang, Q.; Jin, M. S.; Xie, Z. X.; Zheng, L. S. J. Am. Chem. Soc. 2009, 131, 3152–3153.
- [2] Teramura, K.; Oku oka, S.-I.; Yamazoe, S.; Kato, K.; Shishido, T.; Tanaka, T. J. Phys. Chem. C 2008, 112, 8495–8498.
- [3] Yamashita, H.; Harada, M.; Misaka, J.; Takeuchi, M.; Ichihashi, Y.; Goto F.; Ishida, M.; Sasaki, T.; Anpo, M. J. Synchrotron Rad. 2001, 8, 569–571
- [4] Kim, H. G.; Hwang, D. W.; Lee, J. S. J. Am. Chem. Soc. 2004, 126, 8912–8913.
- [5] O'Hayre, R.; Nanu, M.; Schoonman, J.; Goossens, A.; Wang, Q.; Gratzel, M. Adv. Funct. Mater. 2006, 16, 1566–1576.
- [6] Itzhaik, Y.; Niiitso o, O.; Page, M.; Hodes, G. J. Phys. Chem. C 2009, 113, 4254–4256.
- [7] Shankar, K.; Bandara, J.; Paulos e, M.; Wietasch, H.; Varghese, O. K.; Mor, G. K.; LaTempa, T. J.; Thelakkat, M.; Grimes, C. A. Nano Lett. 2008, 8, 1654–1659.
- [8] D.V. Bavykin, A.N. Kulak, V.V. Shvalagin, N.S. Andryushina, O.L. Stroyuk, Photocatalytic properties of rutile nanoparticles obtained via low temperature route from titanate nanotubes, Journal of Photochemistry and Photobiology A 218 (2011) 231–238.
- [9] H.G. Bang, J.K. Chung, R.Y. Jung, S.Y. Park, Effect of acetic acid in TiO<sub>2</sub> paste on the performance of dye-sensitized solar cells, Ceramics International 38 (2012) S511–S515
- [10] N.H.N. Yusoff, M.J. Ghazali, M.C. Isa, A.R. Daud, A. Muchtar, Effects of powder size and metallic bonding layer on corrosion behaviour of plasma-sprayed Al<sub>2</sub>O<sub>3</sub>–13% TiO<sub>2</sub> coated mild steel in fresh tropical seawater, Ceramics International 39 (2013) 2527–2533.
- [11] S. Mohammadi, H. Abdizadeh, M.R. Golobostanfard, Effect of niobium doping on opto-electronic properties of sol-gel based nanostructured indium tin oxide thinfilms, Ceramics International 39 (2013) 4391–4398.
- [12] X.L. Bal, B. Xie, N. Pan, X.P. Wang, H.Q. Wang, Novel threedimensional dandelion-like TiO<sub>2</sub> structure with high photocatalytic activity, Journal of Solid State Chemistry 181 (2008) 450–456.
- [13] X.X. Ren, G.L. Zhao, H. Li, W. Wu, G.R. Han, The effect of different pH modifier on formation of CdS nanoparticles, Journal of Alloys and Compounds 465 (2008) 534–539.
- [14] J. Zhou, G.L. Zhao, J.J. Yang, G.R. Han, Diphenylthiocarbazone (dithizone)-assisted solvothermal synthesis and optical properties of one-dimensional CdS nanostructures, Journal of Alloys and Compounds 509 (2011) 6731–6735.
- [15] Y.X. Li, Y.F. Hu, S.Q. Peng, G.X. Lu, S.B. Li, Synthesis of CdS nanorods by an ethylenediamine assisted hydrothermal method for photocatalytic hydrogen evolution, Journal of Physical Chemistry C 113 (2009) 9352–9358.
- [16] Zhou, W.; Liu, X.; Cui, J.; Liu, D.; Li, J.; Jiang, H.; Wang, J.; Liu, H. CrystEngComm 2011, 13, 4557–4563.
- [17] Bavykin, D. V.; Gordeev, S. N.; Moskalenko, A. V.; Lapkin, A.A.; Walsh, F. C. J. Phys. Chem. B 2005, 109, 8565.
- [18] Meng, X.-D.; Wang, D.-Z.; Liu, J.-H.; Zhang, S.-Y. Mater. Res. Bull. 2004, 39, 2163.
- [19] LI F B, LI X Z, HOU M F, CHEAH K W, CHOY W C H. Enhanced photocatalytic activity of Ce<sup>3+</sup>-TiO<sub>2</sub> for 2-mercaptobenzothiazole degradation in aqueous suspension for odour control [J]. Appl Catal A, 2005, 285: 181–189.
- [20] YU Jia-guo, Wang Guo-hong, CHENG Bei, ZHOU Ming-hua. Effects of hydrothermal temperature and time on the photocatalytic activity and microstructures of bimodal mesoporous TiO<sub>2</sub> powders [J]. Appl Catal B, 2007, 69: 171–180.
- [21] S. Mubeen, G. Hernandez-Sosa, D. Moses, J. Lee and M. Moskovits, Plasmonic Photosensitization of a Wide Band Gap Semiconductor: Converting Plasmons to Charge Carriers, Nano Lett. 11, 5548–5552, 2011